

*Supplement of*

## **Versatile soil gas concentration and isotope monitoring: optimization and integration of novel soil gas probes with online trace gas detection**

Juliana Gil-Loaiza<sup>1</sup>, Joseph R. Roscioli<sup>2</sup>, Joanne H. Shorter<sup>2</sup>, Till H.M. Volkmann<sup>3,4</sup>, Wei-Ren Ng<sup>3</sup>, Jordan E. Krechmer<sup>2</sup>, Laura K. Meredith<sup>1,3,\*</sup>

<sup>1</sup> School of Natural Resources and the Environment, University of Arizona, Tucson, AZ, 85721, USA

<sup>2</sup> Aerodyne Research Inc., Billerica, MA, 01821, USA

<sup>3</sup> Biosphere 2, University of Arizona, Oracle, AZ, 85623, USA

<sup>4</sup> Applied Intelligence, Accenture, Kronberg im Taunus, Hesse, 61476, Germany.

*Correspondence to:* Laura K. Meredith [laurameredith@email.arizona.edu](mailto:laurameredith@email.arizona.edu)

### **Contents of this file**

Figures S1 to S4

Tables S1 to S3

References

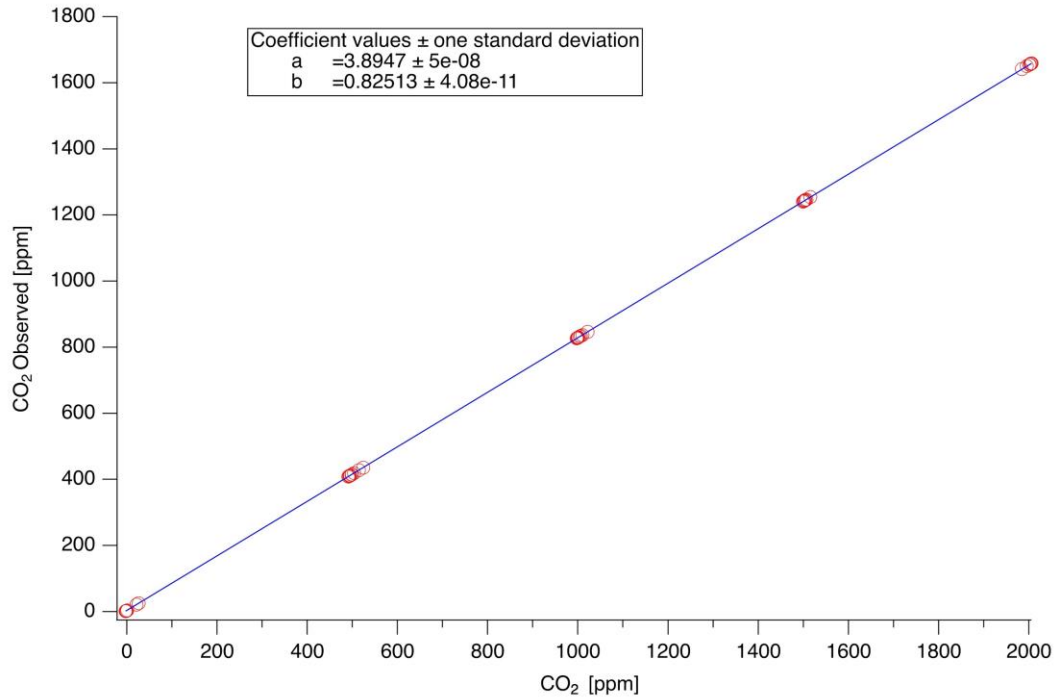


**Figure S1.** Calibration of absolute concentration of CO<sub>2</sub> in silica matrix (System 1 Dual) between observed and controlled dilution mixtures using linear regression relationship

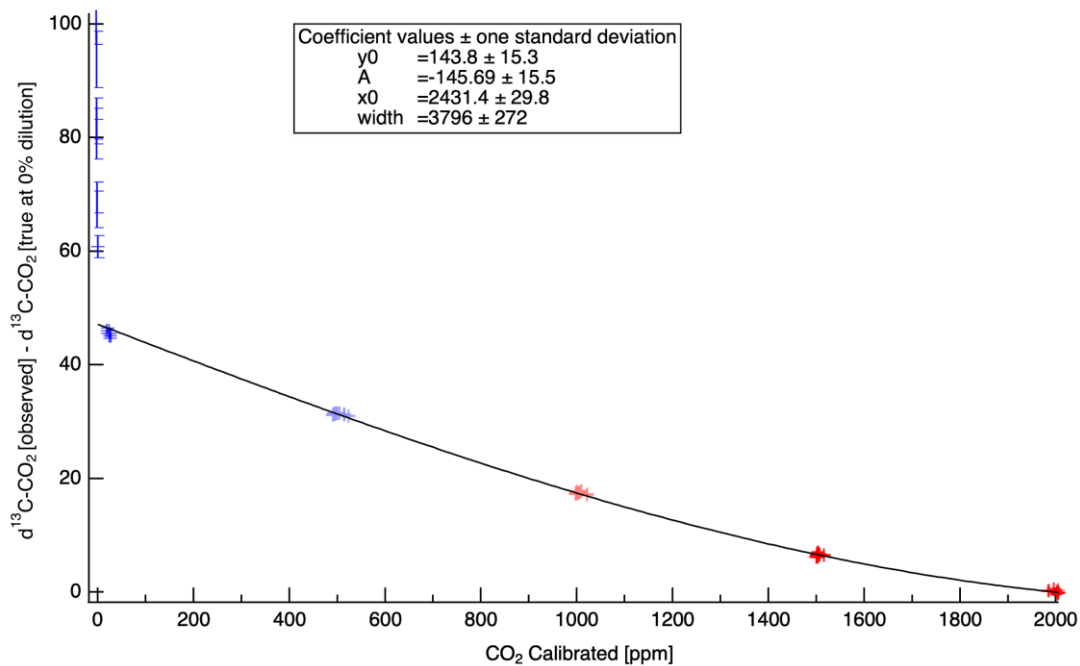


**Figure S2.** Δ<sup>13</sup>C-CO<sub>2</sub> calibration from the concentration dependent relationship of dual δ<sup>13</sup>C-CO<sub>2</sub> vs observed [CO<sub>2</sub>]. The Gaussian equation was used to fit the relationship between (δ<sup>13</sup>C-CO<sub>2</sub> observed - δ<sup>13</sup>C-CO<sub>2</sub> true and CO<sub>2</sub> concentration. δ<sup>13</sup>C-CO<sub>2</sub> calibration offset calibration curve was used to correct observations.

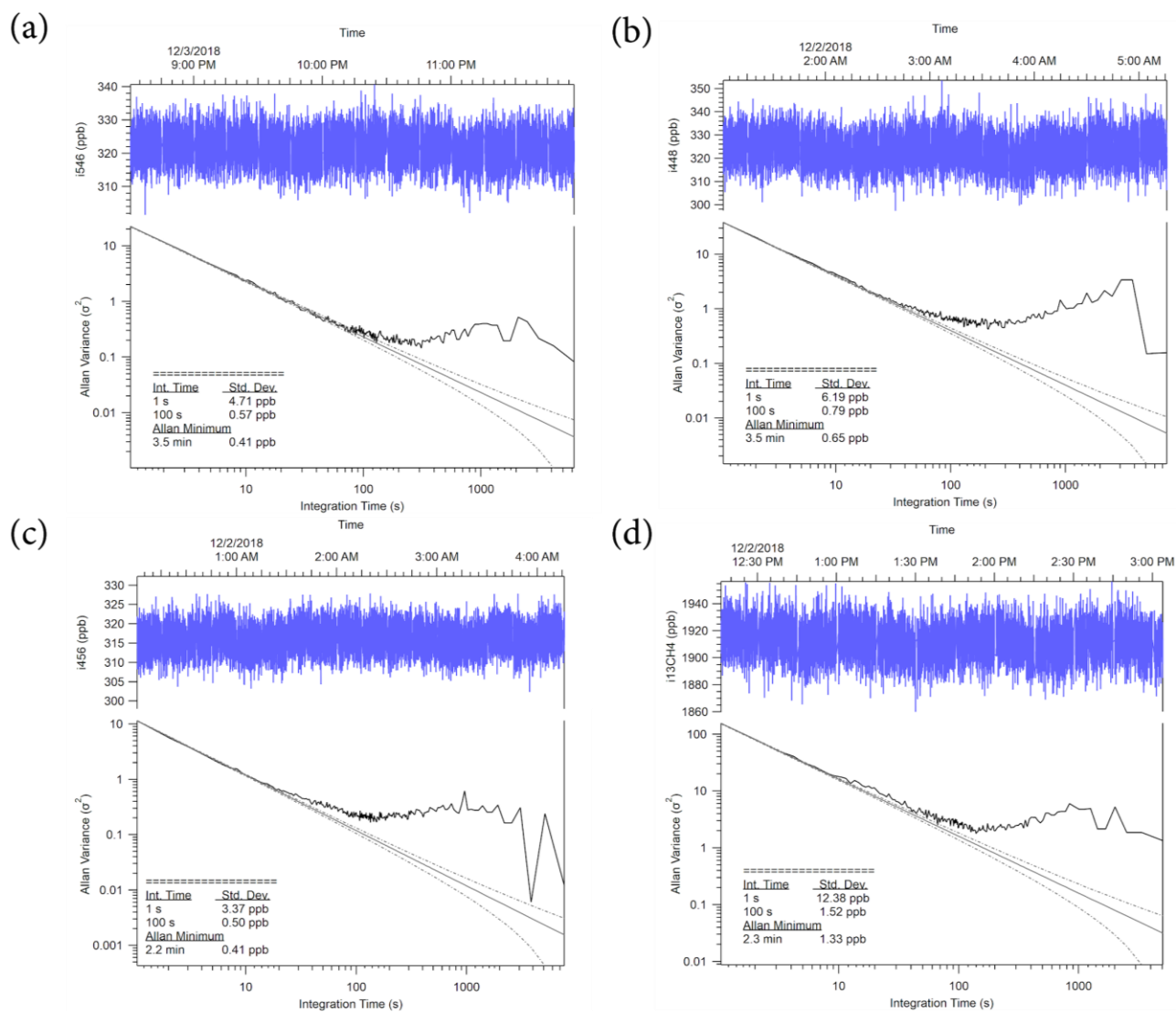


**Figure S3.** Allan-Werle plots of precision for individual minor isotopes  $\text{N}_2\text{O}$  456 and 546 (top), 448 and  $^{13}\text{C-CH}_4$  (bottom). Precision for  $\square$  456 = 1.3 per mil,  $\square$  456 = 1.4 permil,  $\square$  448 = 2.2 per mil, and  $\square$   $^{13}\text{C}$  = 0.7 per mil

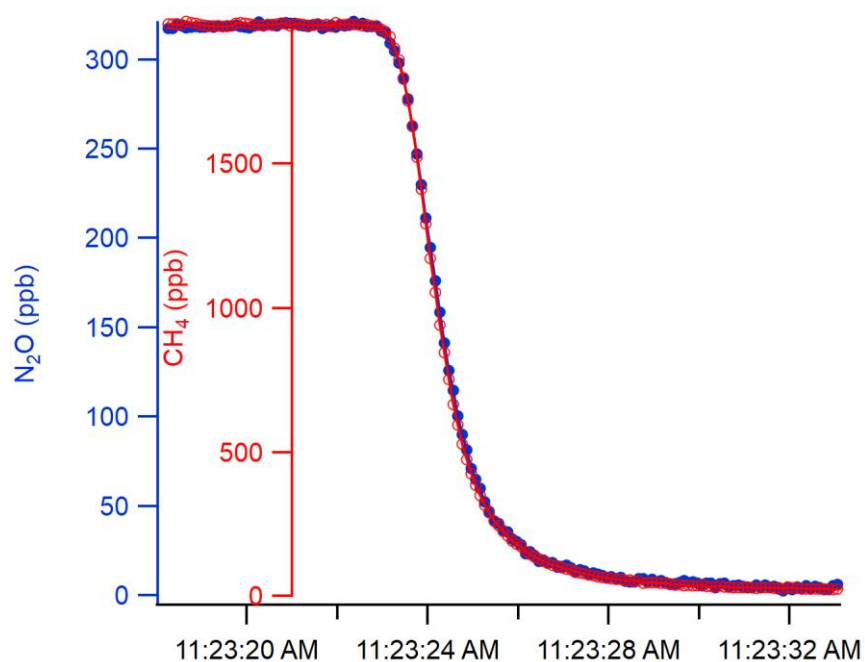


**Figure S4.** Improvement in the time response with the addition of the insert. Time Response of 76m standard cell with insert. P=30 Torr, flow 1 slpm.

**Table S1.** Soil matrix description and particle size distribution

| Type of Matrix                   | Soil ID        | Vendor                  | Particle size distribution (units)  | Type of soil   |
|----------------------------------|----------------|-------------------------|---|--|
| <b>Granusil 4095<sup>1</sup></b> | Silica         | Covia Corporation       | 8 (0%), 16 (0.28%), 20 (27.66%), 30 (52.55%), 40 (15.99%), 50 (3.22%), 70 (0.22%), 100 (0.04%), 140 (0.02%), 200 (0.28%) <sup>a</sup> | High purity industrial quartz, Hardness (Mohs) 7.0, Moisture content <0.1%.                            |
| <b>Type of Soil</b>              | <b>Soil ID</b> | <b>Source Site</b>      | <b>Sampling Location</b>  | <b>Properties</b>  |
| <b>Tropical Rainforest</b>       | Soil 1         | Biosphere 2<br>Tropical | Shaded Lowland (dieffenbachia, vine)  | Sandy, silty loam (40-70% sand 36% silt and 30% clay) <sup>b</sup> ; and C:N 8.75; pH 7-8 <sup>c</sup> |
| <b>Tropical Rainforest</b>       | Soil 3         | Rainforest              | South facing terrace (ginger, hibiscus)   |  |

<sup>a</sup> Mesh units ASTM; <sup>b</sup> (Lin et al., 1999) in (Smith et al., 2020); <sup>c</sup> (Van Haren et al., 2005)

**Table S2.** Measurement precision of the 76 m dual TILDAS for N<sub>2</sub>O/CH<sub>4</sub> isotopes

|   | <b>Mixing Ratio<br/>(ppb)</b> | $\square$ (‰) |
|---|-------------------------------|---------------|
| <b><math>\delta^{546}</math> N<sub>2</sub>O</b><br>( <sup>15</sup> N <sup>14</sup> N <sup>16</sup> O) | 0.46                          | 1.4           |
| <b><math>\delta^{456}</math> N<sub>2</sub>O</b><br>( <sup>14</sup> N <sup>15</sup> N <sup>16</sup> O) | 0.42                          | 1.3           |
| <b><math>\delta^{448}</math> N<sub>2</sub>O</b><br>( <sup>14</sup> N <sup>14</sup> N <sup>18</sup> O) | 0.72                          | 2.2           |
| <b><sup>13</sup>C-CH<sub>4</sub></b>  | 1.3                           | 0.7           |

**Table S3.** References used to estimate the 3D map for N<sub>2</sub>O isotopic signatures of bulk  $\delta^{15}\text{N}$  (x-axis),  $\delta^{18}\text{O}$  (y-axis), and site preference (z-axis) (Figure 12b).

| <b>Microbial activity</b> | <b>Reference</b>   |
|---------------------------|--|
| Bacterial Denitrification | (Frame and Casciotti, 2010; Sutka et al., 2006; Toyoda et al., 2005; Zou et al., 2014) |
| Chemodenitrification      | (Jones et al., 2015; Toyoda et al., 2005; Wei et al., 2017)                            |
| Bacterial nitrification   | (Jung et al., 2014; Sutka et al., 2006; Yoshida, 1988)                                 |
| AOA                       | (Hu et al., 2015)  |
| Fungal denitrification    | (Sutka et al., 2008)   |

## References

Frame, C. H. and Casciotti, K. L.: Biogeochemical controls and isotopic signatures of nitrous oxide production by a marine ammonia-oxidizing bacterium, *Biogeosciences*, 7, 2695–2709, 2010.

Hu, H.-W., Chen, D. and He, J.-Z.: Microbial regulation of terrestrial nitrous oxide formation: understanding the biological pathways for prediction of emission rates, *FEMS Microbiol. Rev.*, 39(5), 729–749, 2015.

- Jones, L. C., Peters, B., Lezama Pacheco, J. S., Casciotti, K. L. and Fendorf, S.: Stable isotopes and iron oxide mineral products as markers of chemodenitrification, *Environ. Sci. Technol.*, 49(6), 3444–3452, 2015.
- Jung, M.-Y., Well, R., Min, D., Gieseemann, A., Park, S.-J., Kim, J.-G., Kim, S.-J. and Rhee, S.-K.: Isotopic signatures of N<sub>2</sub>O produced by ammonia-oxidizing archaea from soils, *ISME J.*, 8(5), 1115–1125, 2014.
- Lin, G., Adams, J., Farnsworth, B., Wei, Y., Marino, B. D. V. and Berry, J. A.: Ecosystem carbon exchange in two terrestrial ecosystem mesocosms under changing atmospheric CO<sub>2</sub> concentrations, *Oecologia*, 119(1), 97–108, 1999.
- Smith, M. N., Taylor, T. C., van Haren, J., Rosolem, R., Restrepo-Coupe, N., Adams, J., Wu, J., de Oliveira, R. C., da Silva, R., de Araujo, A. C., de Camargo, P. B., Huxman, T. E. and Saleska, S. R.: Empirical evidence for resilience of tropical forest photosynthesis in a warmer world, *Nat Plants*, 6(10), 1225–1230, 2020.
- Sutka, R. L., Ostrom, N. E., Ostrom, P. H., Breznak, J. A., Gandhi, H., Pitt, A. J. and Li, F.: Distinguishing nitrous oxide production from nitrification and denitrification on the basis of isotopomer abundances, *Appl. Environ. Microbiol.*, 72(1), 638–644, 2006.
- Sutka, R. L., Adams, G. C., Ostrom, N. E. and Ostrom, P. H.: Isotopologue fractionation during N<sub>2</sub>O production by fungal denitrification, *Rapid Commun. Mass Spectrom.*, 22(24), 3989–3996, 2008.
- Toyoda, S., Mutoke, H., Yamagishi, H., Yoshida, N. and Tanji, Y.: Fractionation of N<sub>2</sub>O isotopomers during production by denitrifier, *Soil Biol. Biochem.*, 37(8), 1535–1545, 2005.
- Van Haren, J. L. M., Handley, L. L., Biel, K. Y., Kuddeyarov, V. N., McLain, J. E. T., Martens, D. A. and Colodner, D. C.: Drought-induced nitrous oxide flux dynamics in an enclosed tropical forest, *Glob. Chang. Biol.*, 11(8), 1247–1257, 2005.
- Wei, J., Zhou, M., Vereecken, H. and Brüggemann, N.: Large variability in CO<sub>2</sub> and N<sub>2</sub>O emissions and in <sup>15</sup>N site preference of N<sub>2</sub>O from reactions of nitrite with lignin and its derivatives at different pH, *Rapid Commun. Mass Spectrom.*, 31(16), 1333–1343, 2017.
- Yoshida, N.: <sup>15</sup>N-depleted N<sub>2</sub>O as a product of nitrification, *Nature*, 335(6190), 528–529, 1988.
- Zou, Y., Hirono, Y., Yanai, Y., Hattori, S., Toyoda, S. and Yoshida, N.: Isotopomer analysis of nitrous oxide accumulated in soil cultivated with tea (*Camellia sinensis*) in Shizuoka, central Japan, *Soil Biol. Biochem.*, 77, 276–291, 2014.